Available online at www.sciencedirect.com

SciVerse ScienceDirect

Procedia Materials Science (2014) 000–000

Procedia Materials Science

www.elsevier.com/locate/procedia

International Congress of Science and Technology of Metallurgy and Materials, SAM - CONAMET 2013

TiO_2 Coatings in Alkaline Electrolytes Using Anodic Oxidation Technique

Alex Iván Kociubczyk[a,*], María Laura Vera[a,b], Carlos Enrique Schvezov[a,b], Eduardo Heredia[c], Alicia Esther Ares[a,b]

[a]*Instituto de Materiales de Misiones - IMAM (CONICET-UNaM), Félix de Azara 1552. (N3300) Posadas-Misiones. Argentina.*
[b]*Facultad de Ciencias Exactas, Químicas y Naturales. Félix de Azara 1552. (N3300) Posadas-Misiones. Argentina.*
[c]*Instituto de Investigaciones Científicas y Técnicas para la Defensa (CITEDEF). (B1603ALO) Villa Martelli-Buenos Aires Argentina*

Abstract

For the construction of a new design of mechanical heart valve a Ti-6Al-4V alloy was selected and coated with TiO_2 due to it corrosion resistance and biocompatibility. A required feature on surfaces in contact with blood it is a low level of roughness (Ra ≤ 50 nm) that not favor the formation of blood clots. One technique that can be used to obtain smooth coatings of TiO_2 is the electrochemical anodic oxidation technique using pre-spark oxidation voltage. The phenomenon of spark produces porous oxides and roughness higher than desired. The beginning of the spark voltage depends on the electrolyte used. The present work compares the coatings obtained by anodic oxidation of the Ti-6Al-4V alloy applying different voltages (from 10V to 50V), using as electrolyte an aqueous based alkaline solutions of NaOH and KOH, at different concentrations (0.1M, 1M and 2M) and $Ca(OH)_2$ at a concentration of 0.02 M, using a constant current of 50mA to achieve the desired voltage. Morphological analysis of the different oxides is performed using optical microscopy, and roughness measurements using a profilometer. The phases present were analyzed by X-ray diffraction technique with a glancing angle of 1º. By varying the applied voltage coatings of different interference colors were obtained. The morphology and roughness of the obtained oxides varied according to the applied voltage in each experience. With KOH and NaOH 1M the spark occurred at 46V and 41V, respectively. The start voltage of the spark decreased to 34V and 29V, respectively, when the electrolyte concentration increase from 1M to 2M. In pre-spark conditions oxides were of an average roughness of 22 nm. After the spark, the oxides became with roughness of 700 nm, limiting the oxidation conditions for the desired application. Anatase and rutile phases were not detected in the coatings, which would be amorphous or with crystalline fractions undetectable by XRD.

"*Keywords*: Titanium, TiO_2, Ti-6Al-4V; Alkaline Electrolytes; Anodic Oxidation"

* Corresponding author. Tel.: +54-376-442-2186; fax: +54-376-442-5414.
E-mail address: akociubczyk@gmail.com

Selection and peer-review under responsibility of the scientific committee of SAM - CONAMET 2013.

1. Introduction

For the construction of a new mechanical heart valve design, a Ti-6Al-4V alloy, called Tigrade 5, ASTMB367, was selected for its good formability, and machinability, corrosion resistance and biocompatibility [Amerio (2006)]. These last two properties are mainly due to the formation, at room temperature, of TiO_2 natural oxide, which can reach a thickness of 2 to 10 nm. However, this natural coating surface has poor mechanical properties, such as low hardness, and low wear and abrasion resistance [Leyens and Manfres (2003), Lutjering and Williams (2007) and Alajdem (1973)]. Therefore, it is convenient to coat the alloy with a layer ofTiO_2 with controlled dimensions and characteristics to improve its performance.

Some of the characteristics required by coatings that should be in contact with blood are the homogeneity and a low level of roughness (Ra ≤ 50 nm), so that they interact the least possible with blood cells, in order not to promote blood clots (thrombosis) [Amerio et al (2006)]. Another property that influences the bio and hemo compatibility of TiO_2 coatings is their crystalline structure. At low pressure, TiO_2 can present three crystalline phases: anatase, rutile orbrookite. According to the literature, both amorphous phases, such as anatase and rutile would be biocompatibles. Some authors argue that the decreasing order of biocompatibility ofTiO_2 phases isrutile>anatase>amorphous [Maitz et al (2003)]. For this reason, the choice of crystalline coatings would be preferable for the intended application.

One technique that can be used to obtain homogeneousTiO_2 coatings with low roughness is the electrochemical anodic oxidation technique, with oxidation voltages below the production spark discharge phenomenon which produces porous oxides and a much rougher surface than desired. This phenomenon leads to a variation of the technique known as anodic oxidation with Anodic Spark Deposition by means of which porous oxides several microns thick can be obtained [Vera et al. (2009) and Songa et al (2009)]. The voltage at which the spark starts varies with the nature and concentration of the electrolyte employed [Sul et al (2001), Liu et al (2004), Kuromoto et al (2007) and Vera (2013)]. Also, this phenomenon is associated with the production of crystalline coatings [Diamanti (2007), Vera (2013)].

From the above, the primary objective of the present work is to define appropriate conditions (type of electrolyte, concentration and applied voltage) to obtain smooth and uniform coatings of TiO_2 by anodic oxidation of Ti-6Al-4V alloy in alkaline electrolytes, to be used in the construction of cardiovascular devices. Further, this research aims at analyzing the structure of the coatings obtained and the response of current density versus time for each voltage applied in relation to the phenomena during the oxidations.

2. Experimental

As substrates to performing oxidations (2 cm x 1cm x 0.2 cm) samples of Ti-6Al-4V alloy metallographically prepared were used by following these steps: cleaning and cutting the material, mounting or inclusion of a piece in acrylic for manipulation; coarse and fine roughing with SiC abrasive papers of decreasing grain size from # 240 to # 2500; intermediate polishing with 1 micron diamond paste and ethylene glycol, final polishing with silica suspension and peroxide to speculate termination. Once samples were removed from the acrylic, they were cleaned with water and commercial detergent and were sprayed with alcohol and dried with hot air.

Coatings were obtained by JMB CC-LPS-360DD source of DC power supply, which is a source of two modules where each one can work with a current of 0 - 3 A and voltages from 0 to 60 V or be connected in series and / or parallel. The source was connected to an electrochemical cell, consisting of a platinum cathode and an anode of the material to oxidize, immersed in a corresponding alkaline electrolyte.

Various alkaline solutions were used as electrolytes: sodium hydroxide (Na OH) and potassium hydroxide (KOH) in concentrations of 0.1M, 1M and 2M and calcium hydroxide ($Ca(OH)_2$) in 0.025M concentration because of low water solubility of this substance.

Each electrolyte oxidation was performed at 10V, 30V and50V. Combining the source a galvanostatic and potentiostatic process of growth was scheduled so that at the beginning a constant current of 50 mA was used until the voltage reached the desired pre-set value which was held constant for 1 minute once it was achieved.

Voltage and current density as a function of oxidation time were recorded in all oxidations. Immediately after the oxidation, test samples were washed in demineralized water and dried with hot air.

Surface observations of the coatings were performed on an optical metallographic Arcano®microscope.

To measure the roughness if the coatings a Time GroupTR200® profilometer was used. Two measurements of samples were performed in each direction (longitudinal and transverse)

The phases present in the coatings were analyzed by X-ray diffraction (XRD) using a Philips PW 3710® diffractometer with a CuKα ($\lambda_{CuK\alpha}$ = 1,5418 Å) wavelength, using a Philips® thin-film accessory allowing operation with a ground-beam geometry with incident angle of 1 °.

3. Results and Discussion

3.1. Analysis of the variation of voltage and current density with oxidation time

Figure 1 shows curves of voltage and current density variations versus time of oxidations carried out with KOH at different concentrations. In Figures 1 (a), (b) and (c) (above), the variation curves of voltage versus time are presented. Also, in Figures 1 (d), (e) and (f) (below) the corresponding variations of the current density versus time are displayed.

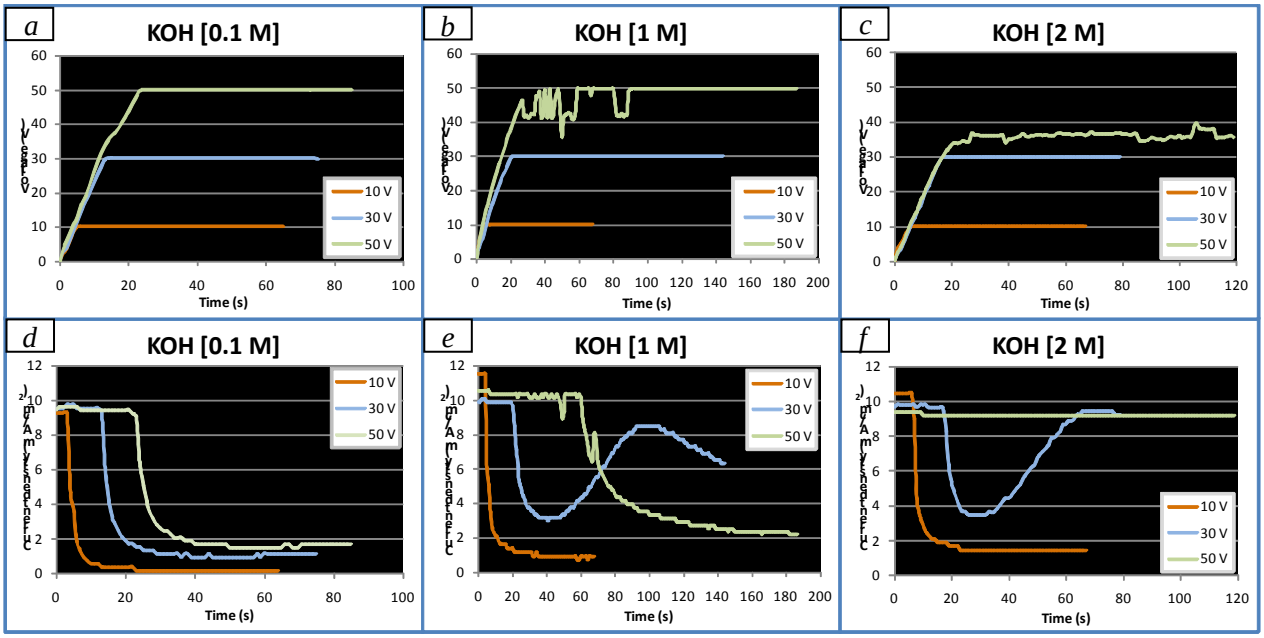

Fig. 1. Voltage variation curves versus time (a, b and c) and current density as a function of time (d, e and f) for 0.1M, 1M and 2M KOH electrolyte.

On curves of voltage variation in Figure 1(a) and current density in Figure 1 (d) corresponding to the oxidations with0.1MKOHat 10V, 30V and50V it can be seen that during the first seconds of oxidation the current density was kept constant, while the voltage gradually increased until the pre set value for each oxidation time. The voltage was kept constant at that value and the current density began to decrease to a value which is substantially constant at the end of the process. This is due to the fact that for a given voltage value, the thickness of the oxide layer increases to a maximum value, also increasing its resistance to current passage. Oxide growth is stopped when the resistance increases to such an extent that the value of the current flowing decreases to a constant value but different from zero. Current flow indicates that reactions and dissolution of the oxide growth still occur. Controlling step in the oxide growth would become the titanium or oxygen diffusion through the coating, so that the speed is reduced significantly compared to the onset of oxidation, and to practical purposes the thickness of the oxide reaches a threshold, indicating that it depends on the applied voltage [Sharma (1992)].

The same behavior is repeated on oxidations performed at 10V with 1M and 2M KOH, as shown in Figures 1 (b) and (e) and in Figures 1 (c) and (f), respectively.

In Figures 1(e) and (f), in the curves of current density corresponding to the oxidations with1M and 2MKOH it can be seen at 30V that increasing the current density within a few seconds it was possible to achieve the desired voltage of 30V(Figure 1(b) and (c)). This behaviour may be due to a phenomenon called *breakdown*, which is the point at which the electric field (between the internal and external interfaces of the oxide) is so high that cannot be supported along the entire thickness, and therefore which produces oxide dielectric breakdown in some places resulting in localized cracks and pores, causing decrease in strength and hence increased current density [Kuromoto (et al) (2007)].

In experiments with1M and 2MKOH in which the voltage was preset at50V it can be seen that the voltage did not remain constant with time (Figure 1(b) and (c)). Experimentally, this coincided with the onset of electrical discharges with chip on the anode that occurred due to dielectric breakdown of the film described previously (breakdown). The high potential difference between the cathode and anode caused that established arcing between the different parts of the coating, resulting in localized spots of micro-plasma that produced an increased of current density [Diamanti (et al) (2010)], not stabilized as oxidations, produced at lower voltages. This intermittency was due to break cycles-bare substrate-oxidation [Vera (2013)]. This phenomenon began to spark with1MKOH with 46Vand2MKOH with 34V. When working with the highest concentration (2M) spark phenomenon was constant and prevented to reach the preset voltage of 50V as shown in the corresponding curve in Figure 1(c).

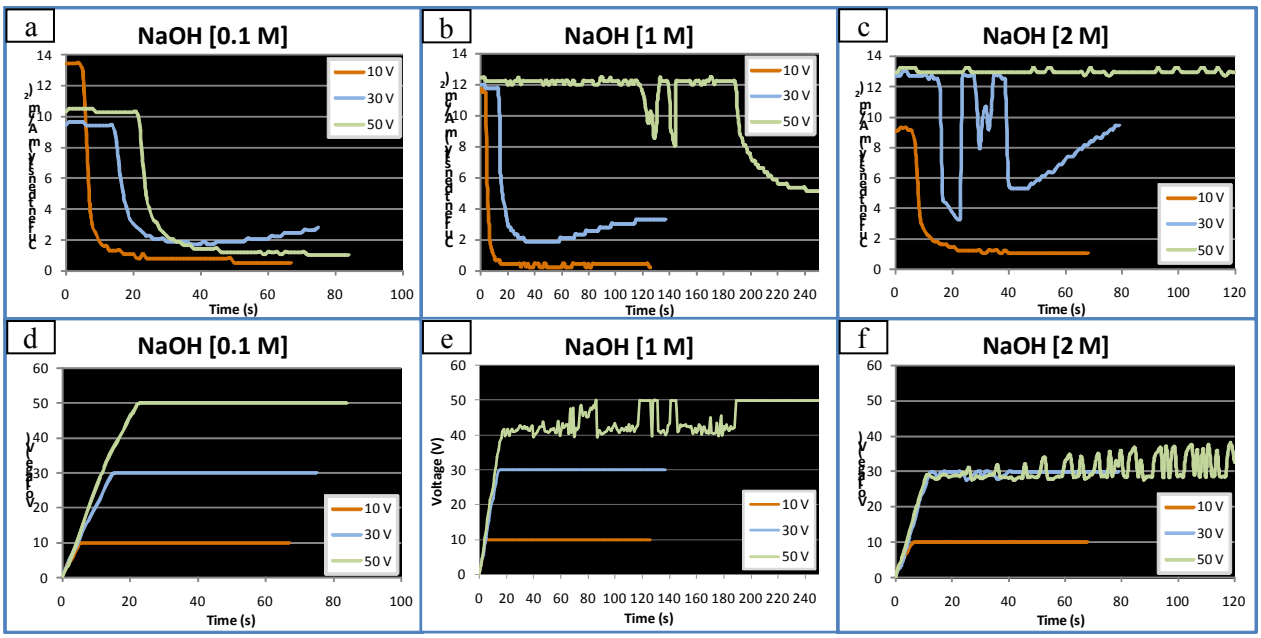

Fig. 2. Voltage variation curves versus time (a, b and c) and current density as a function of time (d, e and f) for 0.1M, 1M and 2M NaOH electrolyte.

Figure2 shows the variation curves of voltage and current density over time for different concentrations of NaOH. Figures 2 (a), (b) and (c) above, present the variation of voltage curves versus time. In Figures 2 (d), (e) and (f) below the corresponding variations of the current density as a function time are displayed. Figures 2(a) and (d), corresponding to the oxidations performed at 10V, 30V and50Vwith0.1MNaOH, followed the characteristic behavior of potentiostatic growth of anodic oxide previously described to oxidations conducted at the same voltages with 0.1MKOH. Figure 1(a) and (d) above also holds to oxidations conducted at 10Vwith 1M NaOH and 2MNaOH.

In Figures 2(b) and (e), in the curves for the oxidation to 30Vwith 1M NaOH similar results as obtained and described for the same voltage with 1MKOH (Figures 1(b) and(e)), in which the breakdown causes localized cracking and consequent increase in the current density, may be observed. In the same Figures 2 (b) and (e), in the curves for the oxidation to 50Vwith 1M NaOH and in Figures 2(c) and (f), in the curves for 30Vand50V it is noted that voltage curves do not remain constant over time. Furthermore, Figures 2(b) and (c) show the curves of 50V do

not reach such value because with 1M NaOH (Figure 2(b)) the spark is started a t41V and 2M NaOH (Figure 2 (c)) the spark began at 29V. In the latter case, the spark was observed even in the experience corresponding to 30 V.

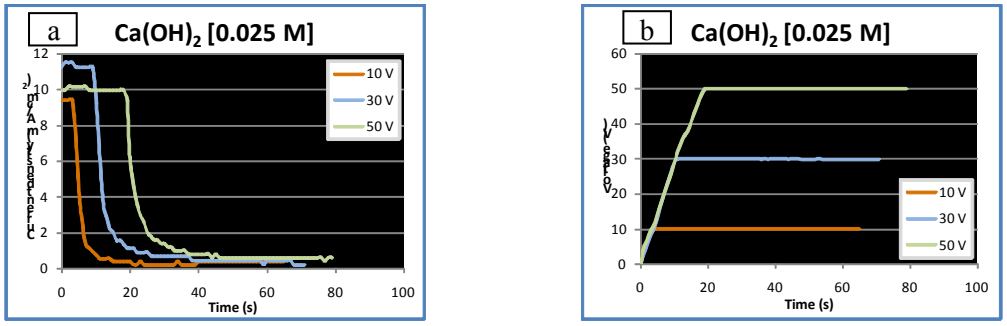

Fig. 3. Voltage variation and current density curves with time corresponding to 0.025M $Ca(OH)_2$.

Figures 3 (a) and (b) show the variation curves of voltage and current density versus time for 0.025M $Ca(OH)_2$, which follow the characteristic behavior of anodic oxide growth describing potentiostatic oxidations performed previously with 0.1M KOH (Figure 1(a) and (d)) and was also observed in the oxidations performed with 0.1M NaOH (Figure 2(a) and (d)).

Table 1 clearly shows the decrease in the spark starting voltage with increasing concentration of the alkaline electrolyte used.

Table 1. Oxidation voltage of five samples in different electrolytes.

Electrolytes	KOH			NaOH			$Ca(OH)_2$
Concentration [M]	0.1	1	2	0.1	1	2	0.025
Beginning of the spark voltage *[V]*	> 50	46	34	> 50	41	29	> 50

3.2. Color and morphology of coatings

In Figures 4, 5 and 6shows the optical micrographs of coatings obtained with KOH, NaOH and $Ca(OH)_2$ respectively, with different electrolyte concentrations and voltages oxidation. It is noted that different interference colors obtained depending mainly on the applied voltage. In previous works the same authors of the present work, it has been shown that there is a direct relationship between color and coating thickness [Vera et al (2009) and Vera (2013)].

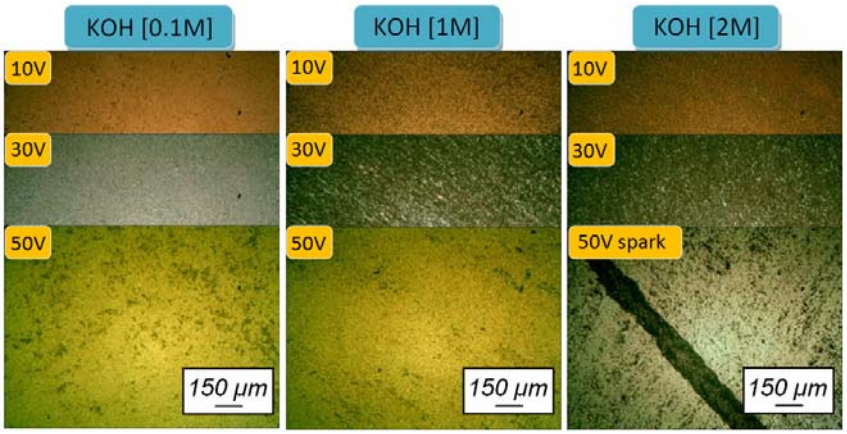

Fig. 4. Micrographs of coatings obtained with KOH.

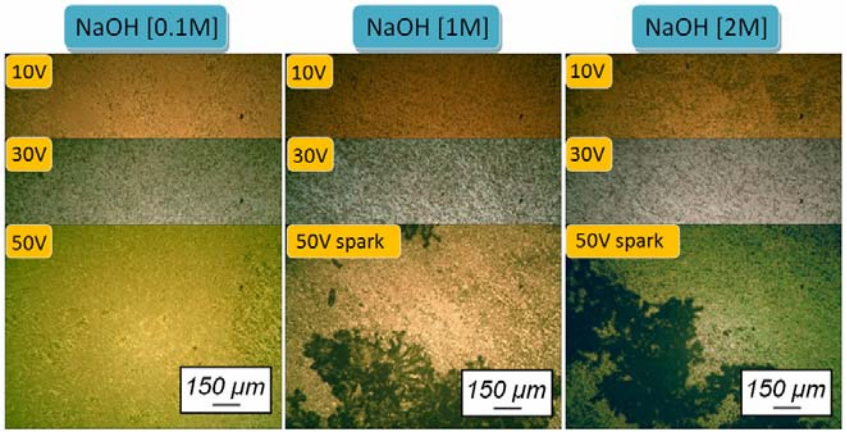

Fig. 5. Micrographs of coatings obtained with NaOH.

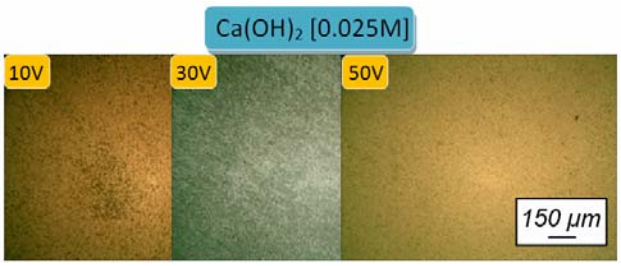

Fig. 6. Micrographs of coatings obtained with Ca $(OH)_2$.

In this figures it can be observed that coatings have a predominantly uniform color with small portions of different tones, quasi-homogeneously distributed over the surface. This staining pattern may be attributed to grow oxides of different thickness over grains with different crystal orientations of α and β phases of Ti-6Al-4V alloy employed as substrate [Vera (2013)]. Beyond small in homogeneities of colors, related to substrate texture, color uniformity of coatings over the whole of each sample is noteworthy, including the edges thereof, so that it highlights the absence variations in the thickness due to edge effects.

The colors obtained for each voltage are identical to those reported in the literature for oxidations performed on the same substrate using H_2SO_4as electrolyte [Vera et al (2008)] and over pure commercial titanium (1 ASTM grade) using alkaline electrolytes as studied here [Sul et al (2001)].

This shows that for the experiments carried out with the same type of electrolyte, at the same voltage and varying

the concentration of the electrolyte, the interference colors obtained are slightly intensified with increasing concentration. This could be attributed primarily to variations in rates of formation of rust, due to changes in the conductivity of the electrolyte concentration, which can cause a change in the stoichiometry of the oxide. Another reason why the color of the oxide may vary, would be the formation of different fractions of crystal structures, which causes changes in density and refractive index of the oxide films formed [Colaccio et al. (2010) and Sul et al (2001)].

In the micrographs of the oxides obtained with 2MKOH at 50V (Figure4) and 1Mand 2MNaOH at 50V (Figure 5), dark spots on the colored background are observed. That is evidence for the formation of spark, product of located travel of the sparks on the anode surface. It is worth noting the qualitative difference between the localized spark observed in alkaline electrolytes with respect to widespread spark on the entire surface that occurs when using acidic electrolytes, as observed in previous works [Vera (2013), Kuromoto et al (2007)].

Regarding the roughness measurements, the previously polished substrate to oxidation, they showed an average roughness of 20 nm, and once oxidized in conditions of voltage below the spark production, the oxide coatings were of an average roughness of 22nm and coatings obtained under post-spark resulted with a roughness of 700nm (measured in localized areas where there was the spark). These roughness values limit the oxidation conditions for the desired application, that is, the use of pre-spark oxidation conditions.

.

3.3. Structure of coatings

Diffractograms in Figure7 shows that in all the samples analyzed, 0nly peaks corresponding to βand α phases of Ti-6Al-4V (TiG5) appear in all alloy employed as a substrate, whose diffractogram is comparatively placed on the same Figure 7. This may be due to the fact that coatings are amorphous or that the crystalline fraction and / or the thickness of coatings are insufficient to identify crystalline phases by the XRD technique employed.While there is agreement in that the amorphous coatings are also biocompatible [Maitz et al (2003)], several reports indicate that a mixture of anatase and rutile is the most suitable for haemocompatible applications [Huang et al (2003), Schvezov et al (2010)], a reason why we intend to conduct heat treatments coatings obtained in pre-spark that fulfilled preset roughness conditions as a technique to crystallize in anatase and / or rutile phase.

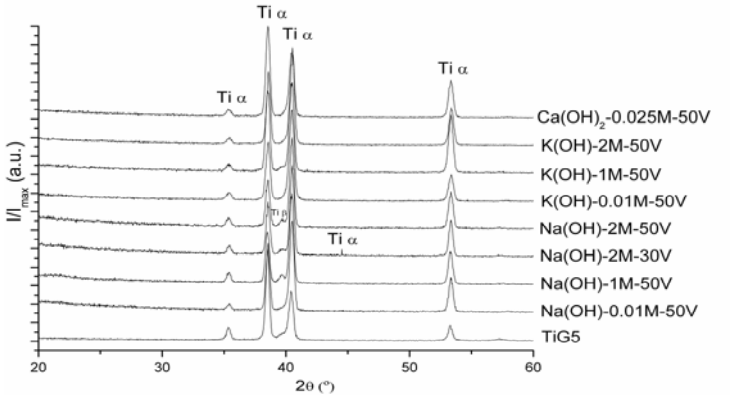

Fig. 7. X-ray diffractograms of samples oxidized with different electrolytes and voltages.

4. Conclusions

The study of anodic oxidation of Ti-6Al-4V alloy in alkaline electrolytes at different concentrations for 1 minute, at constant voltage, yielded the following conclusions:

To obtain homogeneous coatings, amorphous and with low roughness, the voltage to work with is directly related to the type of electrolyte and its concentration, and must be less than the production of spark because this phenomenon causes the appearance of electrical shock sparks at the anode, forming a coating with a high degree of

roughness which would favor the formation of blood clots. These electrical discharges initiated at a certain voltage depending on the electrolyte and its concentration, show that the higher the concentration the lower the voltage at which electrical discharge begins. It was found that the effect of spark discharge is a localized phenomenon to working with these alkaline electrolytes. However, working with low enough voltage so that discharges by sparks do not appear, has resulted in an amorphous coating which reproduces the surface roughness of the substrate and in compliance with the desired values for the application of the manufacture of cardiovascular devices.

5. Acknowledgements

The authors thank to Consejo Nacional de Investigaciones Científicas y Técnicas (CONICET) and Agencia Nacional de Promoción Científica y Tecnológica (ANPCyT) of Argentina, for financing the present research. Alex Iván Kociubczyk thanks to Comité Ejecutivo de Desarrollo e Innovación Tecnológica (CEDIT) for the scholarship.

6. References

Alajdem, A., 1973. Review Anodic Oxidation of Titanium and its Alloys. Journal of Materials Science 8, 688-704.

Amerio, O. N., Rosenberger, M.R., Favilla, P. C., Alterach, M. A., Schvezov C. E., 2006. Prótesis Valvular Cardíaca Trivalva Asociada a Última Generación de Materiales Hemo-Biocompatibles. Revista Argentina de Cirugía Cardiovascular 4, 70 -76.

Colaccio, A. M., Gónzales, C. A., Wendler, P. F., 2010. Influencia de la Concentración del Electrolito en los Recubrimientos de TiO_2 Obtenidos por Oxidación Anódica. Tercer Encuentro de Jóvenes Investigadores en Ciencia y Tecnología de los Materiales, Concepción del Uruguay, Argentina, paper T08-131.

Diamanti, M.V., Pedeferri, M.P., 2007. Effect of Anodic Oxidation Parameters on the Titanium Oxides Formation. Corrosion Science 49, 939-948.

Diamanti, M. V., Bolzoni, F., Ormellese, M., Pérez-Rosales, E. A., Pedeferri, M. P., 2010. Characterisation of Titanium Oxide Films by Potentiodynamic Polarisation and Electrochemical Impedance Spectroscopy. Corrosion Engineering, Science and Technology 45 (6), 428-434.

Huang, N., Yang, P.,. Leng, Y. X, Chen, J. Y., Sun, H., Wang, J., Wang, G. J., Ding, P. D., Xi, T. F., Leng, Y., 2003. Hemocompatibility of Titanium Oxide Films. Biomaterials 24, 2177-2187.

Kuromoto, N., Simão, R., Soares, G., 2007. Titanium Oxide Films Produced on Commercially Pure Titanium by Anodic Oxidation with Different Voltajes. Materials Characterization 58, 114–121.

Leyens, C., Manfres, P., 2003. Titanium and Titanium Alloys: Fundamentals And Applications, Wiley- VCH.

Liu, X., Chub, P. K., Ding, C., 2004. Surface Modification of Titanium, Titanium Alloys, and Related Materials for Biomedical Applications. Materials Science and Engineering R 47, 49–121.

Lutjering, G., Williams, J. C., 2007, "Titanium", Springer.

Maitz, M. F., Pham, M-T., Wieser, E., 2003. Blood Compatibility of Titanium Oxides with Various Crystal Structure and Element Doping. Journal of Biomaterials Applications 17, 303-319.

Schvezov, C.E., Alterach, M.A., Vera, M.L., Rosenberger, M.R., Ares, A.E., 2010. Characteristics of Haemocompatible TiO_2 Nano-Films Produced by the Sol-Gel and Anodic Oxidation Techniques. JOM, a publication of The Minerals, Metals & Materials Society, 84-87.

Sharma, A. K., 1992. Anodizing Titanium for Space Applications. The Solid Films 208, 48-54.

Song, H., Park, S., Jeong, S., Park, Y., 2009. Surface Characteristics and Bioactivity of Oxide Films Formed by Anodic Spark Oxidation on Titanium in Different Electrolytes. Journal of Materials Processing Technology 209, 864–870.

Sul, Y., Johansson, C., Jeong, Y., Albrektsson, T., 2001. The Electrochemical Oxide Growth Behaviour on Titanium in Acid and Alkaline Electrolytes. Medical Engineering & Physics 23, 329–346

Vera, M. L., Ares, A. E., Lamas, D. G., Schvezov, C. E., 2008. Preparación y Caracterización de Recubrimientos de Dióxido de Titanio Obtenidos por Oxidación Anodica de la Aleación Ti-6Al-4V. Primeros Resultados. Anales AFA 20, 178-183.

Vera, M. L., Ares, A. E., Rosenberger, M. R., Lamas, D. G., Schvezov, C. E., 2009. Determinación por Reflectometría de Rayos X del Espesor de Recubrimientos de TiO_2 Obtenidos por Oxidación Anódica. Anales AFA 21, 174-178.

Vera, M. L., 2013. Obtención y Caracterización de Películas Hemocompatibles de TiO_2. Tesis Doctoral, Instituto de Tecnología Jorge Sabato, UNSAM-CNEA, Buenos Aires, Argentina.